

UCSF

UC San Francisco Previously Published Works

Title

LARP1 haploinsufficiency is associated with an autosomal dominant neurodevelopmental disorder.

Permalink

<https://escholarship.org/uc/item/4nc359j3>

Journal

HGG Advances, 5(4)

Authors

Chettle, James

Louie, Raymond

Larner, Olivia

et al.

Publication Date

2024-10-10

DOI

10.1016/j.xhgg.2024.100345

Peer reviewed

LARP1 haploinsufficiency is associated with an autosomal dominant neurodevelopmental disorder

James Chettle,^{1,20} Raymond J. Louie,^{2,20,*} Olivia Lerner,³ Robert Best,³ Kevin Chen,⁴ Josephine Morris,¹ Zinaida Dedeic,¹ Anna Childers,² R. Curtis Rogers,² Barbara R. DuPont,² Cindy Skinner,² Sébastien Küry,^{5,6} Kevin Uguen,⁷ Marc Planes,⁷ Danielle Monteil,⁸ Megan Li,⁹ Aviva Eliyahu,^{10,11} Lior Greenbaum,^{10,11,12} Nofar Mor,¹³ Thomas Besnard,^{5,6} Bertrand Isidor,^{5,6} Benjamin Cogné,^{5,6} Alyssa Blesson,¹⁴ Anne Comi,¹⁴ Ingrid M. Wentzensen,¹⁵ Blake Vuocolo,¹⁶ Seema R. Lalani,¹⁶ Roberta Sierra,¹⁶ Lori Berry,¹⁶ Kent Carter,¹⁷ Stephan J. Sanders,^{18,19,20} and Sarah P. Blagden^{1,20,21,*}

Summary

Autism spectrum disorder (ASD) is a neurodevelopmental disorder (NDD) that affects approximately 4% of males and 1% of females in the United States. While causes of ASD are multi-factorial, single rare genetic variants contribute to around 20% of cases. Here, we report a case series of seven unrelated probands (6 males, 1 female) with ASD or another variable NDD phenotype attributed to *de novo* heterozygous loss of function or missense variants in the gene *LARP1* (La ribonucleoprotein 1). *LARP1* encodes an RNA-binding protein that post-transcriptionally regulates the stability and translation of thousands of mRNAs, including those regulating cellular metabolism and metabolic plasticity. Using lymphocytes collected and immortalized from an index proband who carries a truncating variant in one allele of *LARP1*, we demonstrated that lower cellular levels of LARP1 protein cause reduced rates of aerobic respiration and glycolysis. As expression of *LARP1* increases during neurodevelopment, with higher levels in neurons and astrocytes, we propose that *LARP1* haploinsufficiency contributes to ASD or related NDDs through attenuated metabolic activity in the developing fetal brain.

Introduction

Neurodevelopmental disorders (NDDs) are defined in the fifth edition of the Diagnostic and Statistical Manual of Mental Disorders (DSM-5) as early-onset developmental deficits (e.g., failure to achieve cognitive, motor, or social milestones) that lead to long-term impairments. Such deficits may be limited (e.g., specific learning disorders) or generalized (e.g., global developmental delay). Many are highly heritable; where specific genetic loci have been identified, they often overlap between multiple NDDs.¹ Autism spectrum disorder (ASD) is diagnosed in 2.8% of children and is an NDD defined by impairments in social communication and the presence of restricted or repetitive behaviors or interests.² Although common genetic variants observed in over 1% of the population account for the majority of variance in the ASD trait, single rare genetic variants contribute to about 20% of individuals affected by ASD.³ These are often rare *de novo* variants, frequently occurring

in genes with roles in transcriptional or messenger RNA (mRNA) regulation or neuronal communication,⁴ although some biallelic variants affect genes with roles in metabolism.^{5,6} It is estimated that many more genes associated with NDDs and ASD remain to be discovered.⁴

LARP1 (La ribonucleoprotein 1; translational regulator; ENSG00000155506; HGNC:29531), located on chromosome 5 (at 5q33.2), encodes the LARP1 (UniProt: Q6PKG0) RNA-binding protein (RBP)⁷ and is highly conserved across evolution. Large-scale human population reference databases reveal dramatically fewer than expected protein-truncating variants (PTVs) in *LARP1*, suggesting strong selective pressure with the loss of one functioning copy (haploinsufficiency, pLI = 1.0, LEOUF = 0.17 [top decile], gnomAD v.2) and from missense variation (gnomAD v.2 missense Z score = 3.07).⁸ Cohorts of individuals with developmental delays and ASD have identified two *de novo* PTVs and four *de novo* missense variants, which did not meet genome-wide significance in either

¹Department of Oncology, University of Oxford, Oxford, UK; ²Greenwood Genetic Center, Greenwood, SC, USA; ³University of South Carolina School of Medicine Greenville, Greenville, SC, USA; ⁴Yale University, New Haven, CT, USA; ⁵Nantes Université, CHU Nantes, Service de Génétique Médicale, 44000 Nantes, France; ⁶Nantes Université, CHU Nantes, CNRS, INSERM, L'institut du thorax, 44000 Nantes, France; ⁷Service de Génétique Médicale et Biologie de la Reproduction, CHRU de Brest, Brest, France; ⁸Naval Medical Center Portsmouth, Portsmouth, VA, USA; ⁹Invitae, San Francisco Corp., San Francisco, CA, USA; ¹⁰The Danek Gertner Institute of Human Genetics, Sheba Medical Center, Tel Hashomer, Israel; ¹¹Sackler Faculty of Medicine, Tel Aviv University, Tel Aviv, Israel; ¹²The Joseph Sagol Neuroscience Center, Sheba Medical Center, Tel Hashomer, Israel; ¹³The Genomic Unit, Sheba Cancer Research Centre, Sheba Medical Center, Tel Hashomer, Israel; ¹⁴Kennedy Krieger Institute, Baltimore, MD, USA; ¹⁵GeneDx, Gaithersburg, MD, USA; ¹⁶Baylor College of Medicine, Houston, TX, USA; ¹⁷University of Texas Rio Grande Valley, Edinburg, TX, USA; ¹⁸Institute of Developmental and Regenerative Medicine, Department of Paediatrics, University of Oxford, Oxford, UK; ¹⁹Department of Psychiatry and Behavioral Sciences, UCSF Weill Institute for Neurosciences, University of California, San Francisco, San Francisco, CA, USA

²⁰These authors contributed equally

²¹Lead contact

*Correspondence: rlouie@ggc.org (R.J.L.), sarah.blagden@oncology.ox.ac.uk (S.P.B.)

<https://doi.org/10.1016/j.xhgg.2024.100345>.

© 2024 The Author(s). Published by Elsevier Inc. on behalf of American Society of Human Genetics.

This is an open access article under the CC BY-NC-ND license (<http://creativecommons.org/licenses/by-nc-nd/4.0/>).



cohort.^{4,9} However, a combined analysis suggested that *LARP1* might be associated with NDDs (false discovery rate [FDR] = 0.047). A single *de novo* missense variant was also reported in a cohort of 232 individuals affected by congenital hydrocephalus.¹⁰

Levels of LARP1 protein are aberrantly elevated in cancer cells, where many of its physiological functions were identified.^{11–13} Its activation is dependent on phosphorylation at multiple sites by upstream kinases, including mTOR, CDK1, and Akt/S6K1, whereupon LARP1 selectively binds target mRNAs via its La module and DM15 domain to alter their stability and, hence, their translation efficiency.^{14–16} In this way, LARP1 acts at the point of convergence of afferent signaling cascades to post-transcriptionally regulate specific genes, notably those required for ribosomal biogenesis, cellular metabolism, and survival.^{17,18} Of its metabolic targets, LARP1 binds mRNAs encoding enzymes within the glycolytic, pentose phosphate, lipogenesis, and mitochondrial Krebs and oxidative phosphorylation (OXPHOS) pathways and coordinates switching between glycolytic and mitochondrial metabolism.^{15,17–19} This metabolic plasticity enables cancer cells to survive in conditions of fluctuating nutrient or oxygen availability but is also required for normal cells during embryonic development, cellular stress, or tissue regeneration.^{12,13} Metabolic plasticity is particularly important during embryonic neurogenesis, as brain precursor cells switch between mitochondrial metabolism and glycolysis during key developmental stages.²⁰

Here, we report a case series of seven unrelated probands with heterozygous loss of function or missense *LARP1* variants who present with a variable neurodevelopmental phenotype that includes intellectual disability, hypotonia, motor delay, and/or ASD. The *LARP1* variants were shown to be *de novo* in all seven probands. Using immortalized lymphoblasts obtained from one affected proband (proband 1), we conducted *ex vivo* studies to assess the functional impact of pathogenic *LARP1* alteration. Based on our findings, we propose that by reducing metabolic activity, *LARP1* haploinsufficiency contributes to a newly described autosomal dominant NDD.

Material and methods

Proband cohort

The proband cohort was established using the web-based tool GeneMatcher.²¹ Clinical details were obtained from medical records and provided by their respective institutions. Gene variants were identified via standard laboratory procedures and whole-exome sequencing (WES) or whole-genome sequencing (WGS) performed in diagnostic laboratories. The MANE v.1.2 reference sequence for *LARP1* (ENSG00000155506.19) uses the NM_033551.3/ENST00000518297.6 transcript.

Lymphoblast immortalization

After consent was obtained, lymphoblasts were collected from index proband 1 (see below) and immortalized using a standard Ep-

stein Barr virus [EBV]-transformation technique. Samples were also collected from proband 1's mother and father and similarly immortalized for comparison. *LARP1* was sequenced in all cell lines. Lymphoblasts were maintained in RPMI-1640 (Sigma R8758) with 15% FBS and 1% antibiotic/antimycotic (Sigma A5955) at 37°C (5% CO₂).

CRISPR-Cas9 knockout of LARP1 in HEK293T cells

LARP1 knockout generation in HEK293T cells was performed using Edit-R CRISPR-Cas9 Gene Engineering by transducing with All-in-One Lentiviral sgRNA particles (Dharmacon, source clone IDs: VSGHSOH_28505935, VSGHSOH_28704059, and VSGHSOH_28730675). After lentiviral transduction, cells were selected by growth in puromycin (10 µg/mL), and individual clones were expanded and validated for successful knockout of *LARP1* by western blotting. HEK293T cells were maintained in RPMI (Thermo Scientific, 11875093) supplemented with 10% Fetal Bovine Serum (FBS) and 1% penicillin/streptomycin (15140122) at 37°C (5% CO₂).

LARP1 expression vector transfection

The *LARP1* expression vector was prepared by cloning full length *LARP1* (encoding the 1,096 amino acid isoform, UniProtKB/Swiss-Prot: Q6PKG0.2) was cloned into the expression vector pcDNA4/HisMax A (Thermo Scientific, V86420). Site-directed mutagenesis was performed to generate a *LARP1* expression construct with c.2164dupA (chr5:154,803,344:A:AA, GRCh38), confirmed by sequencing. Transfection was performed with Fugene6 (Promega) using a 3:1 ratio of Fugene6 to plasmid and 2 µg plasmid per well of a 6-well plate. Successful expression of the wild-type and genetic variant constructs were validated by western blotting.

mRNA and protein quantitation

mRNA levels of individual genes were measured by quantitative reverse transcription polymerase chain reaction (RT-PCR) and normalized to the levels of *ACTB* mRNA. For quantitative RT-PCR, mRNA was extracted from cells using the GenElute mammalian Total RNA Miniprep Extraction Kit (Merck, RTN70-1KT) and reverse transcribed to synthesize cDNA using the High Capacity cDNA Reverse Transcription Kit (Thermo Scientific, 4368814). mRNA concentrations were equalized by nanodrop prior to reverse transcription. Quantitative PCR was performed using Fast SYBR green master mix (Thermo Scientific, 4385610) on a StepOnePlus Real-Time PCR system. Primer sequences were as follows: *LARP1* N-terminal: (F) GAACCCATTTGACTACCAG, (R) TTGATGTAGTCTTTGAGCAG; *LARP1* C-terminal: (F) CGACACTCAGTGGTAGCAGG, (R) ATTTGGCATCTTCCCGGACA; and *ACTB*: (F) CACCATGGCAATGAGCGGTTC, (R) AGGTCTTTGCGGATGTCCACGT. Western blots were imaged using an Odyssey scanner (Licor), with densitometry analysis performed using ImageStudio software (Licor). The antibodies used in western blotting were *LARP1* N terminus (Abcam, ab86359), *LARP1* C terminus (13708-1-AP), and B-actin (Santa Cruz, sc-47778).

Metabolic and viability assays

Cells were plated onto a Seahorse XFe96 FluxPak plate (Agilent, 102416-100) at a density of 5×10^4 cells per well (lymphoblasts) or 2×10^4 cells per well (HEK293T) for 24 h. On the day of the assay, the medium was replaced with Seahorse XF DMEM medium (pH 7.4) with 5 mM HEPES and supplemented with 5 mM glucose, 5 mM pyruvate, and 4 mM L-glutamine. Oxygen consumption and extracellular acidification rates were measured by Seahorse

XF analyzer and normalized using the Cyquant NF (Thermo Scientific, C35006) cell viability assay to account for differences in cell number.

Results

LARP1 isoform usage in human brain tissue

The long (full length 1,096 amino acid) isoform is generally used for clinical interpretation (MANE transcript NM_033551.3, ENST00000518297.6). To determine whether this is the best transcript for assessing brain-related phenotypes, we assessed exon-level *LARP1* expression in the developing human brain using BrainVar bulk tissue RNA sequencing (RNA-seq) data from 176 postmortem samples of the dorsolateral prefrontal cortex (Figure 1A).²² The long isoform was substantially more highly expressed than the short isoform (NM_001367719.1, ENST00000524248.5), demonstrated by the high levels of expression at the transcriptional start site of the long isoform but not the short isoform (Figure 1B). Dominance of the long isoform in brain tissue was maintained across development, from the early fetal stage through to 6 years and older (Figure 1C).

Proband characteristics

Proband 1 (PTV: *p.Thr722Asnfs*5*)

Proband 1 is a male aged 18 at the time of evaluation. His history included a diagnosis of ASD, language delay, anxiety, and sensory processing disorder and symptoms of muscle cramps after exercise. He did not have intellectual disability (Full-Scale Intelligence Quotient score = 88) or a history of significant motor delays. At the time of his most recent examination, his growth parameter Z scores were height +0.93 and weight +2.11. Other findings include recurring headaches.

Proband 2 (missense: *p.Asp423His*)

Proband 2 is a female aged 19 at the time of evaluation. Prenatally, she was noted to have mild intrauterine growth retardation. She subsequently had delayed motor milestones and did not walk until 19 months of age. An evaluation revealed an intellectual disability, attention-deficit/hyperactivity disorder (ADHD), and hallucinations. Her language development was also significantly delayed, and she was 4 years of age before she spoke using full sentences. Physical examination findings included joint hyperlaxity, high arched palate, exaggerated cubitus valgus, and 2,3 toe cutaneous syndactyly. She also has had recurrent otitis media. At the time of her most recent clinical evaluation, her growth parameters were a height of 155 cm (10th percentile, $Z = -1.4$ SD), a weight of 58 kg (60th percentile, $Z = +2$ SD), and head circumference of 53 cm (10th percentile, $Z = -1$ SD).

Proband 3 (missense: *p.Ala460Pro*)

Proband 3 is a male aged 22 at the time of evaluation. He had a significant history of motor and language delays and hypotonia and began walking at 18–24 months; his first clear

words were spoken at 4–5 years of age. Developmental testing revealed intellectual disability and ASD. There were also concerns for seizure-like activity that were not captured on electroencephalogram (EEG). At the time of his most recent evaluation, his growth parameters were a height of 175.5 cm (43rd percentile, $Z = -0.2$ SD), a weight of 66.7 kg (37th percentile, $Z = -0.34$ SD), and a head circumference of 60 cm (>99th percentile, $Z = +2.1$ SD). No dysmorphic features were noted.

Proband 4 (missense: *p.Glu707Lys*)

Proband 4 is a male aged 11 at the time of evaluation. He had a significant history of delayed motor development and intellectual disability and had been diagnosed with ASD. Neurologic testing revealed ataxia and cerebellar hypoplasia without hypotonia or seizures. At the time of his most recent evaluation, his growth parameters were a height of 131 cm (3rd percentile, $Z = -1.9$ SD), a weight of 26.8 kg (3rd percentile, $Z = -1.9$ SD), and a head circumference of 53 cm (44th percentile, $Z = -0.2$ SD).

Proband 5 (missense: *p.Ile763Phe*)

Proband 5 is a male aged 3 at the time of evaluation. He was referred to genetic counseling due to intellectual disability (developmental quotient [DQ] = 54) and ASD. He also had episodes of febrile and, latterly, non-febrile seizures. At the time of his most recent evaluation, his height was 100 cm (90th percentile, $Z = 1.3$ SD), weight was 15 kg (90th percentile, $Z = 1.3$ SD), and head circumference was 50 cm (60th percentile, $Z = 0.5$ SD). Physical findings included thick eyebrows and long eyelashes.

Proband 6 (2× missense: *p.Asp793Glu and p.Lys819Arg*)

Proband 6 is a male aged 4 at the time of evaluation for global developmental delay. He presented with mild hypotonia and delayed motor milestones. An evaluation also revealed delayed language development. The proband's behavior was described as anxious, without evidence of ASD. The proband has not undergone cognitive testing. Dysmorphic features include small palpebral fissures, protruding columella, and large ears. At the time of most recent evaluation, he had a significant growth delay, with a height of 96.5 cm (2.5th percentile, $Z = -2$ SD), a weight of 12 kg (0.1st percentile, $Z = -3$ SD), and a head circumference of 48 cm (0.8th percentile, $Z = -2.5$ SD).

Proband 7 (missense: *p.Ile558Thr*)

Proband 7 is a male aged 3 with developmental delay at the time of evaluation. He walked at 3 years of age and continues to have significant language delay. Dysmorphic features include bushy eyebrows and prominent ears. Growth parameters showed a weight of 16.4 kg (29th percentile, $Z = -0.6$ SD) and a height of 103 cm (27th percentile, $Z = -0.6$ SD). His fronto-occipital circumference at the age of 18 months was assessed to be 52 cm (93rd percentile, $Z = 1.5$ SD). Additionally, he was noted to have mild hydronephrosis.

Summary of *LARP1* variants

All seven probands were identified based on novel heterozygous variants in the *LARP1* gene detected by genetic

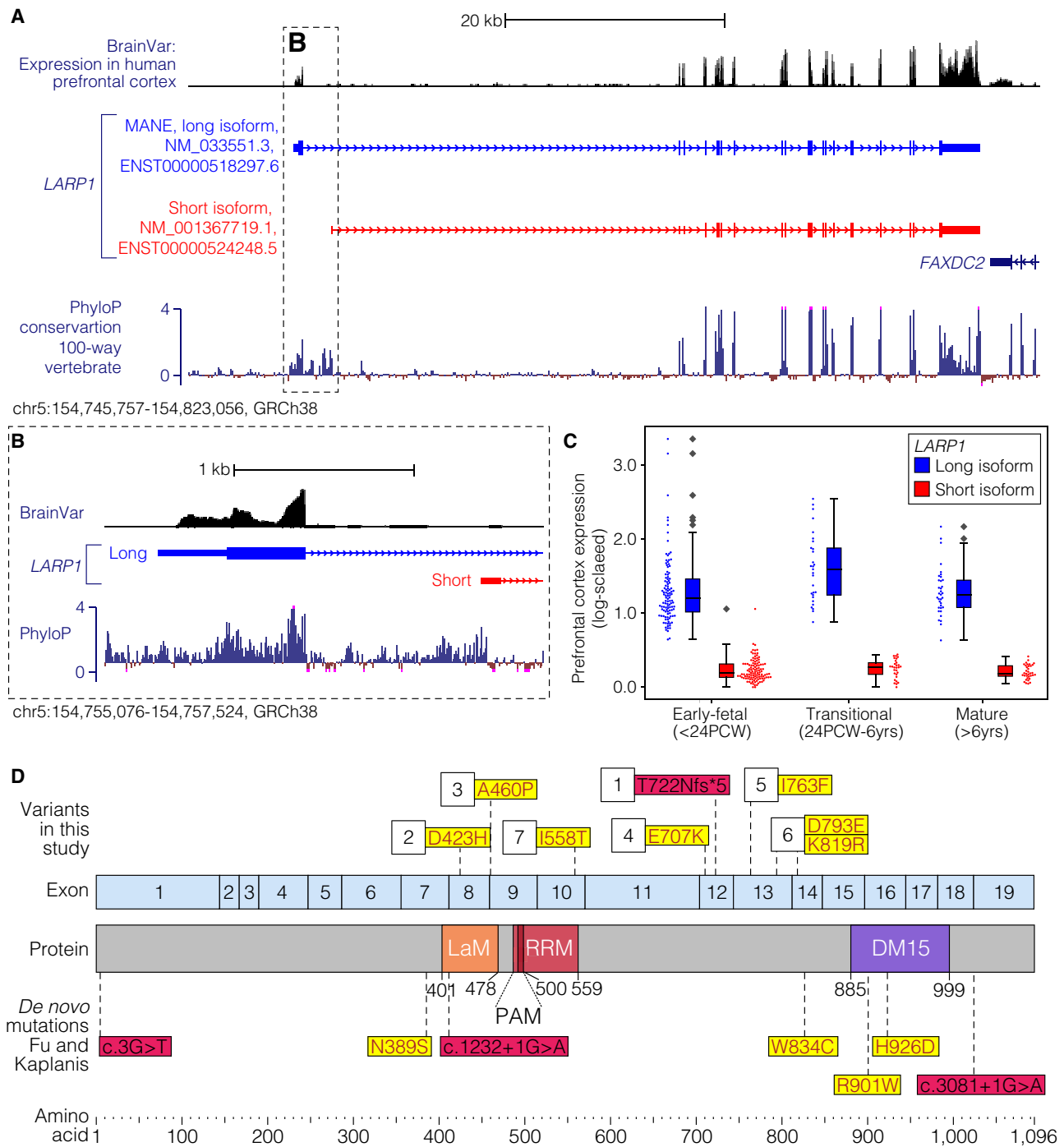


Figure 1. LARP1 isoforms and pathogenic variants in probands

(A) *LARP1* is a positive strand gene on chromosome 5 with two major isoforms: long/full length (blue), in which the first three exons encode amino acids, and short (red), in which the first three exons are non-coding. Mean expression across 176 postmortem human prefrontal cortex samples is shown at the top (BrainVar²²), and 100-way conservation across species (PhyloP) is shown at the bottom. (B) Zoomed-in view of the differing transcription start sites from (A). (C) Expression of the first exon from the long and short isoforms of *LARP1* are shown for each of the 176 samples split into three developmental stages (PCW, post-conceptual weeks). (D) Schematic representation of *LARP1* protein and the variation by proband (numbered above) described in this study and *de novo* genetic variants in developmental delay and ASD cohorts.^{4,9} LaM, La motif; RRM, RNA recognition motif; PAM, PABP-interacting motif; DM15, *LARP1*-specific HEAT-like tandem repeat region.

sequencing (Table 1). Six had missense changes in coding regions of the gene. The remaining subject (proband 1) had a PTV due to a single-nucleotide insertion leading to a

frameshift and premature stop codon (Figure 1D). Probands 2, 3, and 7 had missense variants in the region encoding the highly conserved La module, required for RNA

Table 1. Summary of pathogenic LARP1 variants and clinical features of the seven probands in this study

	Proband 1	Proband 2	Proband 3	Proband 4	Proband 5	Proband 6	Proband 7	Totals
Age at time of exome analysis	18	19	22	11	3	5	3	–
Sex	male	female	male	male	male	male	male	6:1 (male: female)
LARP1 variant (NM_033551.3)	c.2164dup (p.Thr722AsnfsTer5)	c.1267G>C (p.Asp423His)	c.1378G>C (p.Ala460Pro)	c.2119G>A (p.Glu707Lys)	c.2287A>T (p.Ile763Phe)	c.2379C>G (p.Asp793Glu); c.2456A>G (p.Lys819Arg)	c.1673T>C (p.Ile558Thr)	–
Genomic coordinates of mutation (GRCh38/hg38)	chr5:154,803,344	chr5:154,795,209	chr5:154,799,591	chr5: 154,803,299	chr5:154,803,593	chr5:154,803,685 and chr5:154,804,217	chr5: 154,799,999	–
Inheritance	<i>de novo</i>	<i>de novo</i>	<i>de novo</i>	<i>de novo</i>	<i>de novo</i>	<i>de novo</i>	<i>de novo</i>	7/7 <i>de novo</i>
Growth parameters								
Height	183 cm/82%tile (Z = 0.93 SD)	155 cm/10%tile (Z = –1 SD)	175.5 cm/43%tile (–0.2 SD)	131 cm/3%tile (Z = –1.9 SD)	100 cm/90%tile (Z = 1.3 SD)	96.5 cm/2.5%tile (Z = –2 SD)	103 cm/27 %tile (Z = –0.6 SD)	–
Weight	101 kg/98%tile (Z = 2.1 SD)	58 kg/60%tile (Z = +2 SD)	66.7 kg/37%tile (–0.3 SD)	27 kg/3%tile (Z = –1.9 SD)	15 kg/90%tile (Z = 1.3 SD)	12 kg/0.1%tile (Z = –3 SD)	16 kg/29 %tile (Z = –0.6 SD)	–
Head Circumference	57 cm/91%tile (Z = 1.3 SD)	53 cm/10%tile (Z = –1 SD)	60 cm/>99%tile (+2.1 SD)	53 cm/44%tile (Z = 0.15 SD)	50 cm/60%tile (Z = 0.5 SD)	48 cm/0.8%tile (Z = –2.5)	52 cm/93%tile (Z = 1.5 SD)	–
Motor delay	–	+	+	+	–	+	+	5/7
Language delay	+	+	+	–	+	+	+	6/7
Intellectual disability	– (FSIQ = 88)	+	+	+	+	not tested	not tested	4/5
Behavioral abnormality	ASD	ADHD, hallucinations	ASD, anxiety	ASD	ASD	anxiety	–	6/7
Hypotonia	+	–	+	not tested	not tested	+ (mild)	not tested	3/4
Seizure concern	–	–	+ (suspected)	not tested	+ (febrile)	–	–	2/6
Facial features	–	–	–	–	thick eyebrows, long eyelashes	small palpebral fissures, protruding columella, large ears	bushy eyebrows, prominent ears, and underdeveloped inferior crus; features resembled father	3/7
Musculoskeletal	muscle cramps	joint hyperlaxity, 2,3 toe cutaneous syndactyly, cubitus valgus	–	–	–	–	–	2/7
Other	headaches	arched palate, recurrent otitis media	–	ataxia, cerebellar hypoplasia	–	–	hypermobility, long digits, heart murmur, mild hydronephrosis	4/7

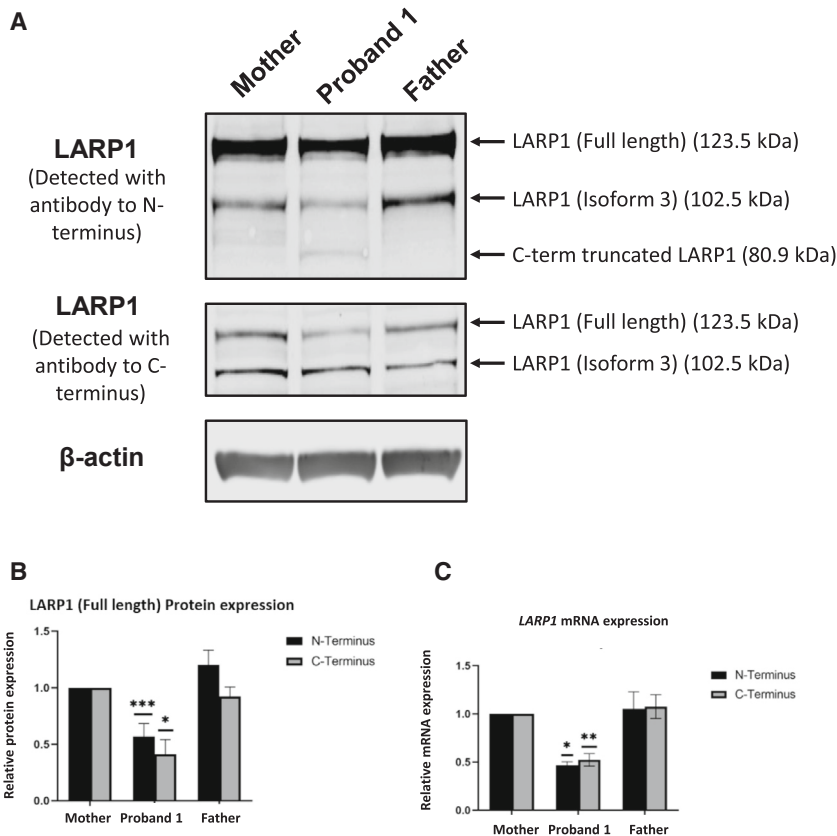


Figure 2. Immortalized lymphoblasts derived from proband 1 express reduced levels of LARP1

(A) Immortalized lymphoblasts derived from proband 1 express ~50% lower levels of full-length LARP1 protein compared with his parents. Immunoblotting was conducted using an antibody raised against human LARP1 amino acids 250–350 (top) and a C-terminal antibody against amino acids 848–1096 (middle). β -Actin was used as a loading control (bottom). A variant protein corresponding to the predicted molecular weight (80.9 kDa) of the C-terminal truncated LARP1 is detected only in proband 1.

(B) The western blot in (A) was quantified by densitometry relative to expression levels in proband 1's mother and confirmed a ~50% decrease in expression levels of LARP1 protein.

(C) *LARP1* mRNA levels were quantified by RT-qPCR using primer pairs corresponding to the N and C termini of *LARP1*. All data were normalized to expression levels in immortalized lymphoblasts from proband 1's mother (*LARP1* wild type). * $p < 0.05$, ** $p < 0.01$, and *** $p < 0.001$ ($n = 3$).

interaction.²³ Additionally, proband 6 had two missense variants (phase unknown) upstream of the DM15 RNA-binding region. All probands had confirmed *de novo* variants. All variants were novel and not reported in ClinVar or the Genome Aggregation Database (gnomAD v.2.1).

While clinical features varied among the probands in this cohort, all had delay in at least one developmental domain. Specifically, of the seven individuals studied in this cohort, language delay was observed in six (6/7) and motor delay in five (5/7). Four had intellectual disability (4/7), and six (6/7) had behavioral issues, including ASD, ADHD, or anxiety. Variable phenotypes include hypotonia (3/4), and three (3/7) had seizures. Of note, the majority were male (6/7), which may be consistent with the preponderance of ASD in males, although this study size is currently too small to determine significance.²⁴

Immortalized lymphoblasts derived from proband 1 express low levels of LARP1 and exhibit reduced metabolism

To characterize the pathogenic variation and the putative truncated protein produced by proband 1, peripheral blood was collected from him and his parents to generate immortalized lymphoblasts. Sequencing confirmed the previously identified *LARP1* c.2164dupA (p.Thr722Asnfs*5) variant alongside a wild-type *LARP1* sequence, indicating that the variant was carried in one allele and, hence, was heterozygous. Notably, lymphoblasts derived from both parents

were shown to be wild type for *LARP1*, indicating that proband 1 carried a *de novo* *LARP1* variant.

Two major *LARP1* isoforms have been described, the full-length “long” isoform encoding a 1,096 amino acid LARP1 protein (NM_033551.3, ENST00000518297.6) and a second “short” 891 amino acid LARP1 isoform (NM_001367719.1, ENST00000524248.5) with an alternative transcription start site that excludes the first coding exon (Figure 1A).²⁵ Hence, LARP1 is observable as a duplex band on western blotting (Figure 1A; Table S1). Lymphoblasts derived from proband 1 had approximately 50% levels of full-length LARP1 protein compared to normal (Figures 2A and 2B) and a protein of approximately 80 kDa corresponding to the predicted molecular weight of the truncated LARP1 protein introduced by the c.2164A duplication (725 amino acids). The levels of *LARP1* mRNA were quantified by qPCR using primer pairs corresponding to the regions of mRNA encoding its N terminus or C terminus. Again, mRNA levels of *LARP1* were significantly lower (~50%) in lymphoblasts from proband 1 compared to those from his parents (Figure 2C). Both the 5' (encoding N terminus) and 3' (encoding C terminus) regions of *LARP1* mRNA were significantly reduced in proband 1. As the 5' region lies upstream of the frameshift, this indicates that mRNA transcribed from the variant allele is likely to be unstable or degraded by nonsense-mediated decay, as no difference in the relative ratio of 5':3' *LARP1* mRNA was observed (Figure 2C).

We next conducted functional comparisons between lymphoblasts from proband 1 and those derived from his unaffected parents. Although proliferation rates were similar (Figure S1), oxygen consumption (indicative of

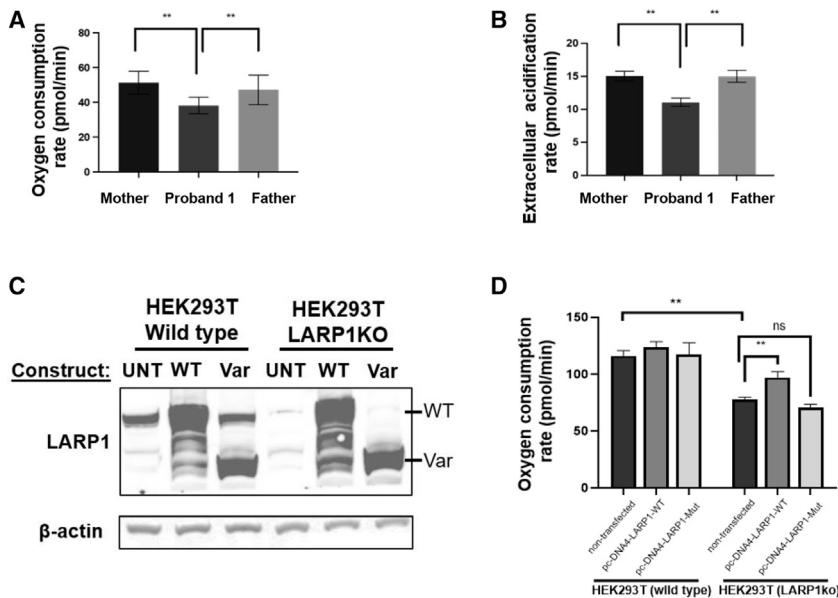


Figure 3. Full-length, but not truncated, *LARP1* promotes cellular metabolism

(A and B) Oxygen consumption rate (A) and extracellular acidification rate (B) of proband 1's lymphoblasts compared to wild-type lymphocytes from his parents. * $p < 0.05$ and ** $p < 0.01$ ($n = 3$).

(C) Wild-type or *LARP1* knockout (*LARP1KO*) HEK293T cells were transfected with expression constructs expressing either wild-type *LARP1* or the truncated variant (Var) of *LARP1* found in proband 1. Successful expression of both constructs was confirmed by western blotting.

(D) Oxygen consumption rate measured by Seahorse assay in wild-type HEK293T and *LARP1KO* cells transfected with wild-type and truncated *LARP1* expression constructs. The low oxygen consumption rate of HEK293T *LARP1KO* cells was partially rescued by the wild type *LARP1* expression construct but not the truncated *LARP1* expression construct.

aerobic respiration) and extracellular acidification rates (indicative of glycolysis) were both significantly reduced in proband 1's cells (Figures 3A and 3B). We then questioned whether both wild-type and truncated *LARP1* expression vectors could rescue the metabolic phenotype associated with *LARP1* loss. Consistent with other cell lines lacking *LARP1*, *LARP1*-null HEK293T cells display lower oxygen consumption rates than wild-type cells, but this phenotype was partially rescued by the expression of wild-type *LARP1* from the transfected expression vector (Figures 3C and 3D). In contrast, the truncated *LARP1* expression vector was unable to rescue oxygen consumption rates despite stable expression. Of note, both the mRNA and protein expressed from the truncated *LARP1* construct were stable, whereas the endogenous mRNA encoding the truncated variant from proband 1 was rapidly degraded. These findings indicate that hemizygous loss of the functional *LARP1* protein from proband 1 was the cause of the reduced metabolism observed in his cells, as the truncated form of *LARP1* lacks the functionality of the full-length protein and, furthermore, is only expressed at a very low level.

Expression of *LARP1* in the brain

To explore the role of *LARP1* in neuronal development, we examined the expression of *LARP1* in the developing human cortex using bulk RNA-seq data from 176 postmortem samples in BrainVar.²² *LARP1* is highly expressed in the cortex from the earliest observation in the middle of the first trimester onwards, with slightly higher postnatal expression (Figure 4A). No differences were observed in expression patterns or levels across the brain regions in the BrainSpan dataset (Figure S2).²⁶ Furthermore, through analysis of a previously published single-cell RNA-seq dataset from the adult human cortex (middle temporal gyrus), *LARP1* was found to be robustly expressed throughout major subclasses of inhibitory and excitatory neurons, with

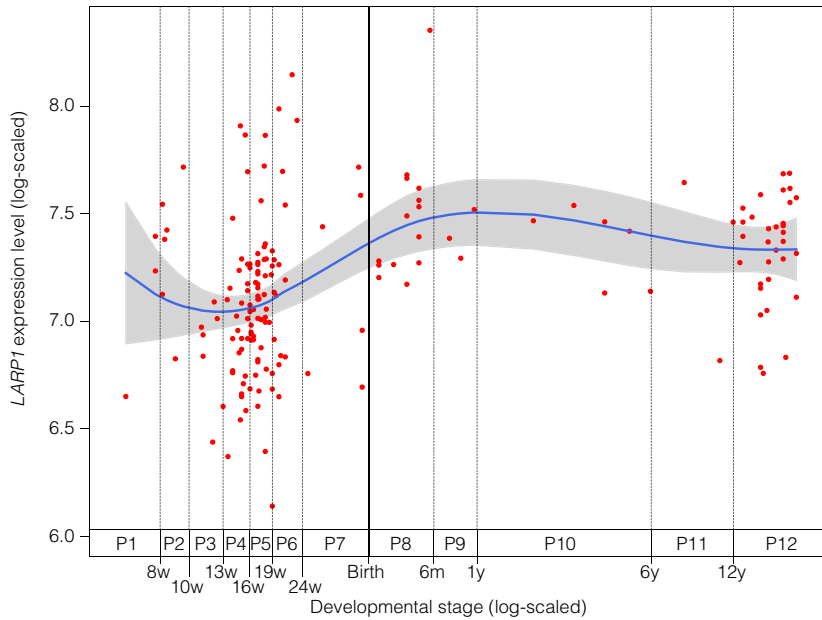
more modest expression in astrocytes, oligodendrocytes, and oligodendrocyte precursor cells.²⁷ The highest expression of *LARP1* was observed in inhibitory *PAX6*-, *LAMP5*-, *VP*-, and *SST*-expressing neurons, alongside substantial expression in multiple classes of excitatory neurons. The timing and cell specificity of *LARP1* expression in the developing brain indicates the importance of precise regulation and may underpin why the observed variants in *LARP1* are associated with NDDs.

Discussion

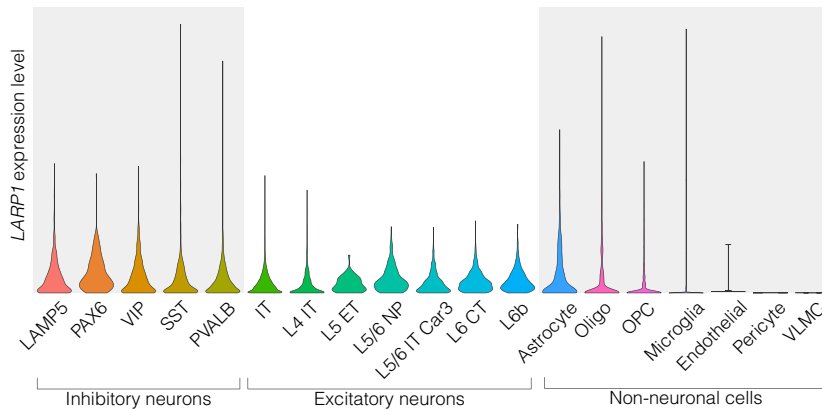
LARP1 is a highly conserved RBP that directly binds and stabilizes essential ribosomal biogenesis, cell survival, and metabolism mRNAs.^{14–16} Although the functional role of *LARP1* in neuronal cells has yet to be established, in cancer cells, the loss of *LARP1* attenuates cell respiration and metabolic plasticity, specifically the ratio of glycolytic to mitochondrial metabolism in response to environmental alterations, such as nutrient depletion.^{28,29}

Here, we describe the first case series of heterozygous variants in *LARP1*, identifying seven unrelated probands with overlapping neurodevelopmental phenotypes. It is noteworthy that an additional *de novo* *LARP1* missense variant (c.2743C>T [p.L915F], CADD score: 26.5) has been reported in a proband with congenital hydrocephalus, raising the possibility of a wider phenotypic spectrum.¹⁰ Testing lymphoblasts obtained from one index proband, we observed a truncated, non-functioning form of *LARP1* protein with normal expression from the remaining wild-type allele. This halving of the total *LARP1* protein dose corresponded to reduced cellular glycolysis and mitochondrial respiration, which was restored *in vitro* upon the re-expression of full-length, but not truncated, *LARP1*, indicating a non-dominant-negative effect.

A *LARP1* expression across development in the human prefrontal cortex



B *LARP1* expression by cell type in the adult human middle temporal gyrus



Systematic analysis of large cohorts of individuals with NDD, augmented by clinical genetic sequencing, has led to the identification of hundreds of associated genes. In these cohorts, *LARP1* is expressed in a cell-specific and time-dependent manner within inhibitory and excitatory neurons in the developing brain from the fetal stage onwards. Consistent with a role in NDDs via haploinsufficiency, *LARP1* is highly constrained in human population cohorts (gnomAD),⁸ highly expressed in the developing brain and in excitatory neurons, and plays a role in mRNA regulation. Combined analysis of these cohort studies supports our smaller cohort observation that variants in *LARP1* can lead to neurodevelopmental delay (FDR = 0.047). This raises the possibility that the onset and location of *LARP1* expression in neurons within the developing brain are tightly regulated. Therefore, sequence variants or dysregulated expression of *LARP1* may attenuate cellular metabolism and impact neurological and synaptic development during critical stages of embryogenesis resulting in clinical features of NDDs.

Several other mRNA-associated genes have already been associated with NDDs, including *FMR1* (fragile

Figure 4. *LARP1* expression across development and by cell type in the human cortex

(A) *LARP1* expression (log₂ counts per million +1) from bulk tissue RNA-seq of the postmortem human prefrontal cortex is shown for 176 samples across brain development (red points) from BrainVar.²² The line represents the LOESS (locally estimated scatterplot smoothing), with the 95% confidence interval shown by the shaded area.

(B) *LARP1* expression is shown from single-cell RNA-seq data of 8 sample of the adult human middle temporal gyrus.²⁷ CT, corticothalamic; ET, extratelencephalic projecting; IT, intratelencephalic projecting; L4, L5, and L6, layers 4, 5, and 6 of the cortex; OPC, oligodendrocyte precursor cells; VLMC, vascular and leptomeningeal cells.

X), *HNRNPU*, *UPF1*, *ELAVL3*, *DHX30*, *DDX23*, *MSI1*, and *SYNCRIP*.^{30–32} Unstable expansion and methylation of CGG trinucleotide repeats within the 5' UTR of *FMR1* cause its silencing and the clinical features of fragile X syndrome (FXS), an inherited developmental disorder causing up to 3% of all cases of ASD. The silencing of *FMR1* causes loss of the protein product FMRP required for post-transcriptional regulation of mRNAs involved in neuronal synaptic plasticity.³³ Other RBPs, such as Pumilio and HuR (ELAV), have also been shown to contribute to neuronal protein synthesis and synaptic plasticity.^{34,35} As synaptic plasticity is increasingly seen as a manifestation of metabolic plasticity and a requirement for normal brain develop-

ment and neuronal plasticity, it is likely that other, similar RBPs may in the future be linked to NDDs, particularly as the use of exome sequencing becomes more widespread.

The identification of the genetic etiology of NDDs not only has relevance for genetic counseling and patient management but can aid the future identification of pathogenic mechanisms and potential therapeutic approaches. Our findings enable us to conclude that *LARP1* genetic variants are predominantly *de novo*, which, together with the phenotypic patterns, supports the association of *LARP1* haploinsufficiency with an autosomal dominant, monogenic, and highly penetrant NDD.

Data and code availability

This study did not generate datasets or code.

Acknowledgments

This work was supported by grants from the National Institute of Mental Health (R01 MH129751 and U01 MH122681 to S.J.S.)

and National Institutes of Health (5UG3TR004047 to S.R.L and B.V).

Author contributions

R.J.L., A.C., R.C.R., B.R.D. and C.S. identified the mutation in proband 1 and R.J.L. collaborated with other centers to identify other probands. J.C. conducted the experimental work, S.J.S. provided in silico data. S.P.B. oversaw the project. S.P.B., S.J.S., J.C. and R.J.C. drafted the manuscript and revisions. All authors contributed to editing and reviewing the manuscript.

Declaration of interests

S.J.S. receives research funding from BioMarin Pharmaceutical. M.L. is an employee and shareholder of Invitae Corp. I.M.W. is an employee of GeneDx, LLC. S.P.B. is a founder and director of RNA Guardian, Ltd.; a patent holder of WO1999062548A9 and WO2016075455A1; has an advisory committee membership to UCB; and has provided consultancy to Simbec Orion, Theolytics, Oxford Drug Discovery, and Ellipses.

Supplemental information

Supplemental information can be found online at <https://doi.org/10.1016/j.xhgg.2024.100345>.

Web resources

BrainSpan, <https://www.brainspan.org/>
BrainVar, <http://www.brainvar.org/>
ClinVar, <https://www.ncbi.nlm.nih.gov/clinvar/>
gnomAd, <https://gnomad.broadinstitute.org/>

Received: January 23, 2024

Accepted: August 21, 2024

References

1. Satterstrom, F.K., Kosmicki, J.A., Wang, J., Breen, M.S., De Rubeis, S., An, J.Y., Peng, M., Collins, R., Grove, J., Klei, L., et al. (2020). Large-Scale Exome Sequencing Study Implicates Both Developmental and Functional Changes in the Neurobiology of Autism. *Cell* 180, 568–584.e23.
2. Maenner, M.J. (2023). Prevalence and Characteristics of Autism Spectrum Disorder Among Children Aged 8 Years — Autism and Developmental Disabilities Monitoring Network, 11 Sites, United States, 2020. *MMWR Surveill. Summ.* 72, 1–14.
3. Klei, L., McClain, L.L., Mahjani, B., Panayidou, K., De Rubeis, S., Grahnat, A.C.S., Karlsson, G., Lu, Y., Melhem, N., Xu, X., et al. (2021). How rare and common risk variation jointly affect liability for autism spectrum disorder. *Mol. Autism.* 12, 66.
4. Fu, J.M., Satterstrom, F.K., Peng, M., Brand, H., Collins, R.L., Dong, S., Wamsley, B., Klei, L., Wang, L., Hao, S.P., et al. (2022). Rare coding variation provides insight into the genetic architecture and phenotypic context of autism. *Nat. Genet.* 54, 1320–1331.
5. Novarino, G., El-Fishawy, P., Kayserili, H., Meguid, N.A., Scott, E.M., Schroth, J., Silhavy, J.L., Kara, M., Khalil, R.O., Ben-Omran, T., et al. (2012). Mutations in BCKD-kinase lead to a potentially treatable form of autism with epilepsy. *Science* 338, 394–397.
6. Doan, R.N., Lim, E.T., De Rubeis, S., Betancur, C., Cutler, D.J., Chiocchetti, A.G., Overman, L.M., Soucy, A., Goetze, S., Autism Sequencing Consortium, et al. (2019). Recessive gene disruptions in autism spectrum disorder. *Nat. Genet.* 51, 1092–1098.
7. Stavrou, C., and Blagden, S. (2015). The La-related proteins, a family with connections to cancer. *Biomolecules* 5, 2701–2722.
8. Lek, M., Karczewski, K.J., Minikel, E.V., Samocha, K.E., Banks, E., Fennell, T., O'Donnell-Luria, A.H., Ware, J.S., Hill, A.J., Cummings, B.B., et al. (2016). Analysis of protein-coding genetic variation in 60,706 humans. *Nature* 536, 285–291.
9. Kaplanis, J., Samocha, K.E., Wiel, L., Zhang, Z., Arvai, K.J., Eberhardt, R.Y., Gallone, G., Lelieveld, S.H., Martin, H.C., McRae, J.F., et al. (2020). Evidence for 28 genetic disorders discovered by combining healthcare and research data. *Nature* 586, 757–762.
10. Jin, S.C., Dong, W., Kundishora, A.J., Panchagnula, S., Moreno-De-Luca, A., Furey, C.G., Allocco, A.A., Walker, R.L., Nelson-Williams, C., Smith, H., et al. (2020). Exome sequencing implicates genetic disruption of prenatal neurogliogenesis in sporadic congenital hydrocephalus. *Nat. Med.* 26, 1754–1765.
11. Desi, N., Tong, Q.Y., Teh, V., Chan, J.J., Zhang, B., Tabatabaeian, H., Tan, H.Q., Kapeli, K., Jin, W., Lim, C.Y., et al. (2022). Global analysis of RNA-binding proteins identifies a positive feedback loop between LARP1 and MYC that promotes tumorigenesis. *Cell. Mol. Life Sci.* 79, 147.
12. Ye, L., Lin, S.T., Mi, Y.S., Liu, Y., Ma, Y., Sun, H.M., Peng, Z.H., and Fan, J.W. (2016). Overexpression of LARP1 predicts poor prognosis of colorectal cancer and is expected to be a potential therapeutic target. *Tumor Biol.* 37, 14585–14594.
13. Hopkins, T.G., Mura, M., Al-Ashtal, H.A., Lahr, R.M., Abd-Latip, N., Sweeney, K., Lu, H., Weir, J., El-Bahrawy, M., Steel, J.H., et al. (2016). The RNA-binding protein LARP1 is a post-transcriptional regulator of survival and tumorigenesis in ovarian cancer. *Nucleic Acids Res.* 44, 1227–1246.
14. Fonseca, B.D., Zakaria, C., Jia, J.J., Graber, T.E., Svitkin, Y., Tahmasebi, S., Healy, D., Hoang, H.D., Jensen, J.M., Diao, I.T., et al. (2015). La-related protein 1 (LARP1) represses terminal oligopyrimidine (TOP) mRNA translation downstream of mTOR complex 1 (mTORC1). *J. Biol. Chem.* 290, 15996–16020. <https://doi.org/10.1074/jbc.M114.621730>.
15. Hong, S., Freeberg, M.A., Han, T., Kamath, A., Yao, Y., Fukuda, T., Suzuki, T., Kim, J.K., and Inoki, K. (2017). LARP1 functions as a molecular switch for mTORC1-mediated translation of an essential class of mRNAs. *Elife* 6, e25237. <https://doi.org/10.7554/eLife.25237>.
16. Haneke, K., Schott, J., Lindner, D., Hollensen, A.K., Damgaard, C.K., Mongis, C., Knop, M., Palm, W., Ruggieri, A., and Stoecklin, G. (2020). CDK1 couples proliferation with protein synthesis. *J. Cell Biol.* 219, e201906147.
17. Mura, M., Hopkins, T.G., Michael, T., Abd-Latip, N., Weir, J., Aboagye, E., Mauri, F., Jameson, C., Sturge, J., Gabra, H., et al. (2015). LARP1 post-transcriptionally regulates mTOR and contributes to cancer progression. *Oncogene* 34, 5025–5036.
18. Smith, E.M., Benbahouche, N.E.H., Morris, K., Wilczynska, A., Gillen, S., Schmidt, T., Meijer, H.A., Jukes-Jones, R., Cain, K.,

- Jones, C., et al. (2021). The mTOR regulated RNA-binding protein LARP1 requires PABPC1 for guided mRNA interaction. *Nucleic Acids Res.* *49*, 458–478.
19. Gentilella, A., Morón-Duran, F.D., Fuentes, P., Zweig-Rocha, G., Riaño-Canalias, F., Pelletier, J., Ruiz, M., Turón, G., Castaño, J., Tauler, A., et al. (2017). Autogenous Control of 5'TOP mRNA Stability by 40S Ribosomes. *Mol. Cell* *67*, 55–70.e4.
 20. Fame, R.M., Shannon, M.L., Chau, K.F., Head, J.P., and Lehtinen, M.K. (2019). A concerted metabolic shift in early forebrain alters the CSF proteome and depends on MYC downregulation for mitochondrial maturation. *Dev. Camb. Engl.* *146*, dev182857.
 21. Sobreira, N., Schiettecatte, F., Valle, D., and Hamosh, A. (2015). GeneMatcher: a matching tool for connecting investigators with an interest in the same gene. *Hum. Mutat.* *36*, 928–930.
 22. Werling, D.M., Pochareddy, S., Choi, J., An, J.Y., Sheppard, B., Peng, M., Li, Z., Dastmalchi, C., Santpere, G., Sousa, A.M.M., et al. (2020). Whole-Genome and RNA Sequencing Reveal Variation and Transcriptomic Coordination in the Developing Human Prefrontal Cortex. *Cell Rep.* *31*, 107489.
 23. Deragon, J.M., and Bousquet-Antonelli, C. (2015). The role of LARP1 in translation and beyond. *Wiley Interdiscip. Rev. RNA* *6*, 399–417. <https://doi.org/10.1002/wrna.1282>.
 24. Loomes, R., Hull, L., and Mandy, W.P.L. (2017). What Is the Male-to-Female Ratio in Autism Spectrum Disorder? A Systematic Review and Meta-Analysis. *J. Am. Acad. Child Adolesc. Psychiatry* *56*, 466–474.
 25. Schwenzler, H., Abdel Mouti, M., Neubert, P., Morris, J., Stockton, J., Bonham, S., Fellermeier, M., Chettle, J., Fischer, R., Beggs, A.D., and Blagden, S.P. (2021). LARP1 isoform expression in human cancer cell lines. *RNA Biol.* *18*, 237–247. <https://doi.org/10.1080/15476286.2020.1744320>.
 26. Li, M., Santpere, G., Imamura Kawasawa, Y., Evgrafov, O.V., Gulden, F.O., Pochareddy, S., Sunkin, S.M., Li, Z., Shin, Y., Zhu, Y., et al. (2018). Integrative functional genomic analysis of human brain development and neuropsychiatric risks. *Science* *362*, eaat7615.
 27. Hodge, R.D., Bakken, T.E., Miller, J.A., Smith, K.A., Barkan, E.R., Graybuck, L.T., Close, J.L., Long, B., Johansen, N., Penn, O., et al. (2019). Conserved cell types with divergent features in human versus mouse cortex. *Nature* *573*, 61–68.
 28. To, T.L., Cuadros, A.M., Shah, H., Hung, W.H.W., Li, Y., Kim, S.H., Rubin, D.H.F., Boe, R.H., Rath, S., Eaton, J.K., et al. (2019). A Compendium of Genetic Modifiers of Mitochondrial Dysfunction Reveals Intra-organelle Buffering. *Cell* *179*, 1222–1238.e17. <https://doi.org/10.1016/j.cell.2019.10.032>.
 29. Chettle, J., Dedeic, Z., Fischer, R., Vendrell, I., Campo, L., Easton, A., Browne, M., Morris, J., Schwenzler, H., Lascaux, P., et al. (2022). LARP1 regulates metabolism and mTORC1 activity in cancer. Preprint at bioRxiv. <https://doi.org/10.1101/2022.09.04.506559>.
 30. Gebauer, F., Schwarzl, T., Valcárcel, J., and Hentze, M.W. (2021). RNA-binding proteins in human genetic disease. *Nat. Rev. Genet.* *22*, 185–198.
 31. Hentze, M.W., Castello, A., Schwarzl, T., and Preiss, T. (2018). A brave new world of RNA-binding proteins. *Nat. Rev. Mol. Cell Biol.* *19*, 327–341. <https://doi.org/10.1038/nrm.2017.130>.
 32. Darnell, J.C., and Richter, J.D. (2012). Cytoplasmic RNA-binding proteins and the control of complex brain function. *Cold Spring Harbor Perspect. Biol.* *4*, a012344.
 33. Zhang, Z., Marro, S.G., Zhang, Y., Arendt, K.L., Patzke, C., Zhou, B., Fair, T., Yang, N., Südhof, T.C., Wernig, M., and Chen, L. (2018). The Fragile X Mutation Impairs Homeostatic Plasticity in Human Neurons by Blocking Synaptic Retinoic-Acid Signaling. *Sci. Transl. Med.* *10*, eaar4338.
 34. Arey, R.N., Kaletsky, R., and Murphy, C.T. (2019). Nervous system-wide profiling of presynaptic mRNAs reveals regulators of associative memory. *Sci. Rep.* *9*, 20314.
 35. Hinman, M.N., and Lou, H. (2008). Diverse molecular functions of Hu proteins. *Cell. Mol. Life Sci.* *65*, 3168–3181.